A Mutation in the *ATP2* Gene Abrogates the Age Asymmetry Between Mother and Daughter Cells of the Yeast *Saccharomyces cerevisiae*

Chi-Yung Lai, Ewa Jaruga, Corina Borghouts and S. Michal Jazwinski[1]

Department of Biochemistry and Molecular Biology, Louisiana State University Health Sciences Center, New Orleans, Louisiana 70112

Manuscript received January 2, 2002
Accepted for publication June 24, 2002

ABSTRACT

The yeast *Saccharomyces cerevisiae* reproduces by asymmetric cell division, or budding. In each cell division, the daughter cell is usually smaller and younger than the mother cell, as defined by the number of divisions it can potentially complete before it dies. Although individual yeast cells have a limited life span, this age asymmetry between mother and daughter ensures that the yeast strain remains immortal. To understand the mechanisms underlying age asymmetry, we have isolated temperature-sensitive mutants that have limited growth capacity. One of these clonal-senescence mutants was in *ATP2*, the gene encoding the β-subunit of mitochondrial F_1, F_0-ATPase. A point mutation in this gene caused a valine-to-isoleucine substitution at the ninetieth amino acid of the mature polypeptide. This mutation did not affect the growth rate on a nonfermentable carbon source. Life-span determinations following temperature shift-down showed that the clonal-senescence phenotype results from a loss of age asymmetry at 36°, such that daughters are born old. It was characterized by a loss of mitochondrial membrane potential followed by the lack of proper segregation of active mitochondria to daughter cells. This was associated with a change in mitochondrial morphology and distribution in the mother cell and ultimately resulted in the generation of cells totally lacking mitochondria. The results indicate that segregation of active mitochondria to daughter cells is important for maintenance of age asymmetry and raise the possibility that mitochondrial dysfunction may be a normal cause of aging. The finding that dysfunctional mitochondria accumulated in yeasts as they aged and the propensity for old mother cells to produce daughters depleted of active mitochondria lend support to this notion. We propose, more generally, that age asymmetry depends on partition of active and undamaged cellular components to the progeny and that this "filter" breaks down with age.

AGING is characterized by the progressive loss of functional and structural integrity of the organism. This process can be seen in most multicellular and in some unicellular organisms such as the budding yeast *Saccharomyces cerevisiae* (Finch 1990). Evolutionary theory indicates that aging is an inevitable outcome for organisms with separate soma and germline (Rose 1991; Jazwinski 1993). Although the theory also suggests that the aging process is likely to involve multiple mechanisms, the commonality of the basic biochemical and cellular organization of all eukaryotes raises the possibility that some of these aging mechanisms might be universal. Genetic studies using model organisms have been instrumental in uncovering the mechanisms of many evolutionarily conserved processes. This approach has also been applied to the mechanisms of aging (for review see Jazwinski 1996). In many instances, this has entailed the examination of mutants displaying phenotypes of relevance to aging. The most straightforward approaches, however, have utilized life-span mutants, because life span is a direct measure of mortality.

Life-span mutants include those with extended as well as those with shortened life spans. Mutants with shortened life spans are frequently encountered. However, the conclusions from analyses of these mutants can be misleading, because any deleterious genetic change can truncate life span whether or not it is associated with normal aging. The isolation of mutants on the basis of extended life span is technically more difficult, and examples of such studies have been rare (Klass 1983; Lin *et al.* 1998). Studies of aging are complicated by the fact that life span can be affected by multiple genetic and environmental factors (for review see Jazwinski 2001).

Some of the key questions in aging concern the differences between germline and soma. Any mechanism invoked to explain the aging of the soma must also be able to accommodate the immortality of the germline. At the level of the organism, the issue is the renewal that occurs at each generation, providing the progeny a fresh start with the potential for a full life span. The aging process of yeast cells best illustrates the cellular and generational asymmetry mentioned above. A daughter cell, or bud, is produced from the mother cell in

[1]*Corresponding author:* Department of Biochemistry and Molecular Biology, Louisiana State University Health Sciences Center, 1901 Perdido St., Box P7-2, New Orleans, LA 70112.
E-mail: sjazwi@lsuhsc.edu

each cell division cycle. In this asymmetric cell division, the mother cell represents the soma and the daughter cell the germline. Individual cells are mortal and can divide only a limited number of times (Mortimer and Johnston 1959; Müller *et al.* 1980). At the end of its life span, the cell stops dividing and dies, perhaps by apoptosis (Laun *et al.* 2001). However, the yeast clone as a whole is immortal. This immortality depends upon the establishment of an age difference between a daughter cell and the mother cell that produces it. Although the daughter cell receives cellular components from the mother cell, it does not inherit the mother cell's age and is always younger than the mother cell. This age asymmetry implies that any substance or process responsible for the aging of mother cells must be carefully isolated from the daughter cells. Disruption of the "filters" that establish this partition should cause a loss of age asymmetry and simultaneous aging of all cells in a yeast population, or "clonal senescence." Clonal senescence is a normal process for primary human fibroblast cell cultures (Smith and Pereira-Smith 1996). Gradual loss of telomeric repeats at the ends of chromosomes has been shown to be responsible for the limited replicative capacity of human fibroblast cells (Bodnar *et al.* 1998). However, yeast telomeres do not shorten with each cell division, and thus telomere shortening cannot be a cause of aging in yeast (D'Mello and Jazwinski 1991).

We decided to isolate and characterize yeast clonal-senescence mutants to gain a better understanding of the establishment of age asymmetry in yeast cell division. Such mutants are also likely to provide clues about the mechanisms of aging. In this article, we report the isolation and characterization of a temperature-sensitive age-asymmetry mutant and identification of the mutated gene. We also examine the cellular mechanism underlying the loss of age asymmetry and clonal senescence, and we provide evidence for the involvement of this mechanism in normal aging.

MATERIALS AND METHODS

Strains and growth media: *S. cerevisiae* strain YPK9 (*MAT***a** *ade2-101*^{ochre} *his3-*Δ*200 leu2-*Δ*1 lys2-801*^{amber} *trp1-*Δ*63 ura3-52*) used for mutant isolation has been described (Kirchman *et al.* 1999). The deletion of the *COX4* gene in strain YPK9 and the induction of the ρ^0 petite in YPK9 to generate strain YSK365 have also been described (Kirchman *et al.* 1999). *S. cerevisiae* strain W303-1A (*MAT***a** *can1-100 ade2-1 his3-11,-15 leu2-3,112 trp1-1 ura3-1*) was obtained from T. Weinert (University of Arizona, Tucson, AZ). Media used in this study were YPD (2% peptone, 1% yeast extract, 2% glucose), YPG (YPD with 3% glycerol instead of glucose), YPR (YPD with 2% raffinose instead of glucose), and complete synthetic medium CM [0.67% yeast nitrogen base without amino acids, 2% glucose, supplemented with adenine (40 μg/ml), arginine (20 μg/ml), aspartic acid (100 μg/ml), glutamic acid (100 μg/ml), histidine (20 μg/ml), leucine (60 μg/ml), lysine (30 μg/ml), methionine (20 μg/ml), phenylalanine (50 μg/ml), serine (375 μg/ml), threonine (200 μg/ml), tryptophan (40 μg/ml), tyrosine (30 μg/ml), valine (150 μg/ml), and uracil (20 μg/ml)]. Individual supplements were omitted from the CM medium for selection of transformants. Solid media contained 2% agar. Media used for life-span determination were adjusted to pH 6.5 with sodium hydroxide prior to sterilization. Anaerobic cultures were grown on YPD plates and the GasPak *Plus* (Becton-Dickinson, San Jose, CA) system was used to maintain an anaerobic environment. Standard genetic and molecular biology methods (Ausubel *et al.* 1994) were used for transformation, Southern blot analysis, strain construction, and genetic analysis throughout this study.

Isolation of clonal-senescence mutants: To isolate mutants with a clonal-senescence phenotype, a logarithmic-phase yeast culture of the wild-type strain YPK9 was mutagenized with ethyl methanesulfonate (EMS) to achieve a kill ratio of ~40%, using procedures described by Winston (1994). Briefly, an overnight culture grown in YPD was washed twice with sterile water and resuspended in 0.1 M sodium phosphate (pH 7.0). A total of 1.7 ml of this cell suspension, containing about 2×10^8 cells, was mixed with 40 μl of EMS and incubated on a shaker at 30°, and 0.2-ml aliquots were removed from the suspension at 20-min intervals and mixed with 8 ml of sterile 5% sodium thiosulfate to stop the reaction. Kill rate at each time point was determined by plating on YPD. Mutagenized cells were washed, resuspended in YPD at 2×10^6 cells/ml, and incubated at 37° for 24 hr. This incubation at the restrictive temperature was meant to reduce the population doubling capacity of any clonal-senescence mutant. After this initial incubation, cells were spread on YPD plates prewarmed to 37° and incubated at 37° for another 24 hr, after which viable cells had grown into microscopic colonies. These colonies were replica plated to fresh YPD plates and transferred to 30° to allow recovery of temperature-sensitive mutants. The original plates were returned to 37° and incubated for another 2 days. At this point, wild-type cells should grow into large colonies at both incubation temperatures, while cells with a clonal-senescence phenotype should remain small at 37°. Clones that formed small or microscopic colonies at 37° but appeared normal at 30° were picked, streaked, and allowed to recover at 30°. About 200 clones were selected for producing small or microscopic colonies at 37° and normal colonies at 30°.

The small size of the selected colonies could be caused by either reduced growth rates or limited replicative capacity at 37°. To distinguish between these two possibilities, isolates were tested by repetitive passaging (serial streaking) at 37°. Cells were streaked on YPD plates and incubated at 37° for 48 hr. From the streaks that grew, cells were streaked onto the next plate or sector. This serial streaking continued with 48 hr of incubation elapsing between each consecutive passage. Isolates that stopped dividing at any point between the first and fifth streaking were considered clonal-senescence mutants and were saved. Only 2 of the initial 200 isolates passed the serial-streaking test. At 37°, isolates CS8 and CS16 had a clonal life span of ~70 and 40 hr, respectively. We chose CS16 for further analysis because of its more drastic phenotype. The remaining isolates were mutants that had reduced growth rates at 37°. These mutants did not stop growing after repeated passages. Cell division cycle mutants would not form detectable colonies at 37° in the mutant isolation scheme and thus did not enter into the analysis.

Life-span determination: Procedures for life-span determination were modified from Egilmez and Jazwinski (1989). A Nikon Labophot 2 microscope with a long working distance objective was used. A ρ^- genotype has been shown to alter yeast life span (Kirchman *et al.* 1999); therefore, starting cultures for life-span determination were grown in YPG medium overnight to eliminate ρ^- cells. To set up a life-span determination experiment, one drop of cells from each strain

was placed on the edge of a freshly made YPD plate. Individual cells were pulled out of the drop and positioned separately from each other. After 2–3 hr of incubation, virgin daughter cells produced by these cells were moved to the center of the plates and lined up in rows. To measure the life spans of these virgin cells, their buds were removed successively and discarded to the edge of the plate with a micromanipulator. The number of buds produced by each cell was recorded. Each experiment included 30–50 cells of each strain. Survival curves were plotted and the significance of differences between life spans of strains was analyzed using the Mann-Whitney test.

Plasmid complementation: A yeast genomic DNA library in plasmid YCp50 (Rose *et al.* 1987) was used for isolation of genes by complementation. Yeast cells were transformed with library DNA, plated on CM-uracil plates, and incubated at 36° for 3 days. Large colonies were picked and streaked to fresh plates, and their ability to grow continuously at 36° was tested by repetitive streaking, as described above. DNA was extracted from transformants capable of continuous growth at 36° using the Easy-DNA kit (Invitrogen, San Diego). Plasmids were isolated from total yeast DNA by transforming *Escherichia coli* HB101 cells, using the Cell-Porator electroporation system (Life Technologies).

Plasmid gap repair and DNA sequencing: One of the plasmids that complemented mutant CS16 was used for plasmid gap repair. This plasmid YP5-SCS1 carries a 10.5-kb insert, containing the entire *ATP2* gene. This plasmid was cut with *Bam*HI to create a 4243-bp gap from 1388 bp upstream to 2855 bp downstream of the translation start site of *ATP2*. CS16 cells were transformed with this gapped plasmid and selected on CM-uracil plates. Plasmids were isolated from Ura^+ colonies and examined by restriction analysis. Those that contained a full-size insert were introduced back into CS16 cells and tested for their ability to complement the clonal-senescence phenotype. Two of the plasmids that failed to complement were purified, and their sequences from the *ATP2*-coding and 150-bp upstream regions were determined, using the Thermo Sequenase kit (Amersham Life Science).

Gene deletion: Deletion of *ATP2* was achieved by γ-transformation (Sikorski and Hieter 1989). A DNA fragment corresponding to the 5′-flanking region of the gene was generated by the polymerase chain reaction (PCR), using the oligonucleotide primers 5′-GTGGAATTCCTTTCACGTGATGCGCTG GGATG-3′ and 5′-GTGAAGCTTCCAATTGGCCTGTCCTGG AGAG-3′. A 3′-flanking fragment was generated using oligonucleotide primers 5′-GGACGCTACTACCGTCTTGTCAAGA GG-3′ and 5′-GTGGAATTCTTCTAGTTGGCTTCAGCGGC-3′. These two fragments were inserted into plasmid pRS403 (Sikorski and Hieter 1989) between the *Bam*HI and *Hin*dIII sites of the polylinker region. Plasmids were linearized with *Eco*RI for transformation. (The *Eco*RI site was introduced by the PCR.) The deletions generated using these plasmids removed the region between nucleotide −177 and nucleotide +1148 relative to the translation initiation site of *ATP2*. Deletions were confirmed by Southern blot analysis.

Telomere analysis: Telomere length was determined by examination of terminal restriction fragments of XY′ telomeres generated by digestion with *Xho*I, essentially according to D'Mello and Jazwinski (1991). DNA (5 μg), isolated with the Easy DNA kit (Invitrogen), was digested overnight with 20 units of *Xho*I (New England BioLabs, Beverley, MA) and separated by electrophoresis in a 0.7% agarose gel in 89 mm Tris, 89 mm boric acid, 2.5 mm EDTA (pH 8.0) for 16 hr at 2 V/cm. The DNA in the gel was denatured and blotted onto a nylon membrane (Nytran, Schleicher & Schuell, Keene, NH). To probe for $G_{1\text{-}3}T$ telomere repeats, the oligomer $(GT)_{20}$ was labeled with digoxigenin (DIG), using [DIG]dUTP and the DIG oligonucleotide tailing kit (Roche Applied Science). The DIG-labeled probe was hybridized to the DNA on the membrane, according to the instructions of the manufacturer. Briefly, filters were prehybridized at 68° in the presence of 0.1 mg/ml poly(A) in 5× SSC (1× SSC is 0.15 m NaCl, 15 mm sodium citrate, pH 7.0), 0.1% SDS, followed by hybridization for 6 hr at 54°. Filters were washed two times for 5 min at the same temperature in 2× SSC, 0.1% SDS, followed by two 5-min washes in 0.1× SSC, 0.1% SDS. Hybridized probe was detected using the DIG High Prime DNA labeling and detection starter kit II using the chemiluminescence substrate disodium 3-(4-methoxyspiro{1,2-dioxetane-3,2′-(5′-chloro)tricyclo [3.3.1.1^{3,7}]decan}-4-yl)phenyl phosphate (CSPD; Roche Applied Science) as substrate, according to the instructions of the supplier. The membrane was incubated with alkaline phosphatase-conjugated anti-DIG antibody (75 milliunits/ml), followed by visualization with CSPD.

Analysis of extrachromosomal ribosomal DNA circles (ERCs): ERCs were detected by Southern blot analysis of total genomic DNA, using a 2-kb fragment of the 35S rRNA gene as a probe, essentially as described (Kim *et al.* 1999). Yeast genomic DNA (20 μg), isolated with the Easy DNA kit (Invitrogen), was separated by electrophoresis on a 0.7% agarose gel in 40 mm Tris-acetate, 2 mm EDTA (pH 8.5) for 24 hr at 1 V/cm. The DNA in the gel was denatured and blotted onto a nylon membrane (Nytran). The blot was prehybridized in 6× SSC, 5× Denhardt's solution (1× Denhardt's solution is 0.02% Ficoll, 0.02% polyvinylpyrrolidone, and 0.02% bovine serum albumin), 0.5% SDS, 50% formamide, and 0.1 mg/ml denatured salmon sperm DNA. Hybridization was for 12 hr at 42° in the same solution. Actin and rDNA probes were labeled with [α-^{32}P] dCTP using the RediPrime II labeling system (Amersham Biosciences) and purified on NICK columns (Amersham Biosciences). The DNA on the membrane was first hybridized with the actin probe for normalization, followed by the rDNA probe. The membrane was washed two times for 15 min in 2× SSC, 0.5% SDS at 42° and then two times for 15 min in 0.1× SSC, 0.2% SDS at 60°. The membrane was analyzed in a phosphorimager (Molecular Dynamics, Sunnyvale, CA), using ImageQuaNT software.

Flow cytometry: Mitochondrial membrane potential was determined in individual cells using 5,5′,6,6′-tetrachloro-1,1,3,3′-tetraethylbenzimidazolcarbocyanine iodide (JC-1; Molecular Probes, Eugene, OR), a cationic dye that exhibits potential-dependent accumulation in mitochondria (Cossarizza *et al.* 1993). The total JC-1 fluorescence per cell reflects both the membrane potential and the mitochondrial mass. The fluorescence of JC-1 was measured in the green channel (λ_{ex} = 490 nm, λ_{em} = 527 nm). Mitochondrial mass was estimated using nonyl acridine orange (NAO; Molecular Probes), which binds cardiolipin regardless of mitochondrial energy state (λ_{ex} = 490 nm, λ_{em} = 518 nm; Benel *et al.* 1989). The replicative age of cells was estimated by staining bud scars that permanently mark the surface of the mother cell after each cell division with Calcofluor White M2R (Sigma, St. Louis; λ_{ex} = 365 nm, λ_{em} = 435 nm; Kim *et al.* 1996).

Exponentially growing cells (1–2 × 10^7/ml) were incubated in the dark with JC-1 (5 μg/ml) or NAO (1 μg/ml) for 20 min in YPD supplemented with 120 μg/ml adenine at either permissive or restrictive temperature. Cells growing on solid medium were scraped off the plates and resuspended in the YPD medium and stained in the same manner. In some cases, the cells were washed with sterile water and stained for an additional 5 min with freshly prepared Calcofluor White M2R (0.1 mg/ml) in the dark at room temperature. The cells were then washed and sonicated for 3 sec prior to flow cytometry. Flow cytometry was carried out using the fluorescence-activated cell sorter Vantage SE (Becton-Dickinson) and the En-

terprise II coherent UV laser (351–364 nm) and Argon laser (488 nm). Fluorescence was detected in the following channels: FL-1 (530/30 nm), FL-2 (585/42 nm), and FL-5 (424/44 nm).

Fluorescence microscopy: Mitochondria were stained in living cells (2×10^7/ml) growing exponentially in YPD supplemented with 120 μg/ml adenine by incubation with 80 nM Mitotracker Red (Molecular Probes) for 15 min in the dark at permissive or restrictive temperature. Cells were washed twice with sterile water, sonicated for 3 sec, placed on a slide freshly precoated with concanavalin A (Sigma), and immediately analyzed using a Nikon Microphot-SA epifluorescence microscope with a ×63 objective. Images were captured with a Micromax CCD camera model ASI 10014 (Princeton Instruments) and analyzed with MetaMorph 4.5 universal imaging software (Advanced Scientific).

Immunofluorescence microscopy: Cells were cultured to late logarithmic phase in YPD at 30° overnight. Portions of the cultures were incubated for 4 hr at 37° or diluted 400-fold in 5 ml YPD and cultured for 24 hr at 37°. Parts of these 24-hr cultures were diluted 40-fold in 5 ml YPD and incubated for an additional 24 hr at 37° to provide the 48-hr samples. All cultures were harvested in late logarithmic phase. Parallel cultures were handled as above, but the temperature was maintained at 30°. The cells from these cultures were immediately processed for indirect immunofluorescence, as described below, and examined using the Nikon Microphot-SA epifluorescence microscope and imaging system described above.

For confocal microscopy, cells were grown on solid YPD medium at 30° or 37° with serial streaking, as described earlier. These cells were scraped from the solid medium and resuspended in 5 ml of YPD for immediate processing for indirect immunofluorescence. The cells were visualized in a Nikon TE300 microscope equipped with a Bioradiance 2100 laser scanning system with a 10-MW krypton/argon laser (Bio-Rad, Hercules, CA), which was operated by LaserSharp 2000 confocal software (Bio-Rad). A total of 200 sections of 0.05 μm each was taken for a 10-μm scanned slice with an optical magnification of ×1000, using a ×100 objective. The final magnification of the cells was ×1500, using a digital zoom of ×1.5.

Cells were fixed by adding 650 μl of 37% formaldehyde (Sigma) and 650 μl of 1 M potassium phosphate (pH 6.5) to 5 ml of yeast culture in YPD. The cells were incubated on a shaker for 2 hr at either 30° or 37°, corresponding to the temperature at which they had been cultured. They were washed two times with 0.1 M potassium phosphate (pH 6.5) and two times with the same buffer containing 1.2 M sorbitol (KPBS). The cells were suspended in 500 μl of KPBS and 2.5 μl of 2-mercaptoethanol and 15 μl Zymolyase 100T (10 mg/ml, U.S. Biologicals) were added. The suspension was incubated at 30° for 30–45 min to digest the cell wall. The cells were then washed two times with KPBS and suspended in 100–500 μl of KPBS, according to the size of the cell pellet. The cell suspension (20 μl) was deposited on a poly-lysine-coated slide (ICN Biomedicals) and left for 10 min. The fluid was removed by aspiration, and the slide was placed in methanol at −20° for 6 min. Then the slide was placed in ice-cold acetone for 30 sec. The slide was briefly air dried and washed 10 times with PBS (1.4 M NaCl, 30 mM KCl, 80 mM Na_2HPO_4, 30 mM KH_2PO_4, pH 7.3). The cells were blocked with PBS-BSA [2 mg bovine serum albumin (BSA)/ml PBS] for 30 min. Porin staining was performed by incubating the slides in a 1:20 dilution of mouse antiporin antibodies (Molecular Probes) in PBS-BSA for 1 hr at room temperature. Slides were washed 10 times with PBS-BSA and then incubated with a fluorescein isothiocyanate-coupled secondary antibody (goat anti-mouse, Molecular Probes) at 1:32 dilution for 2 hr. Slides were washed 10 times as above and mounted in ProLong Antifade (Molecular Probes).

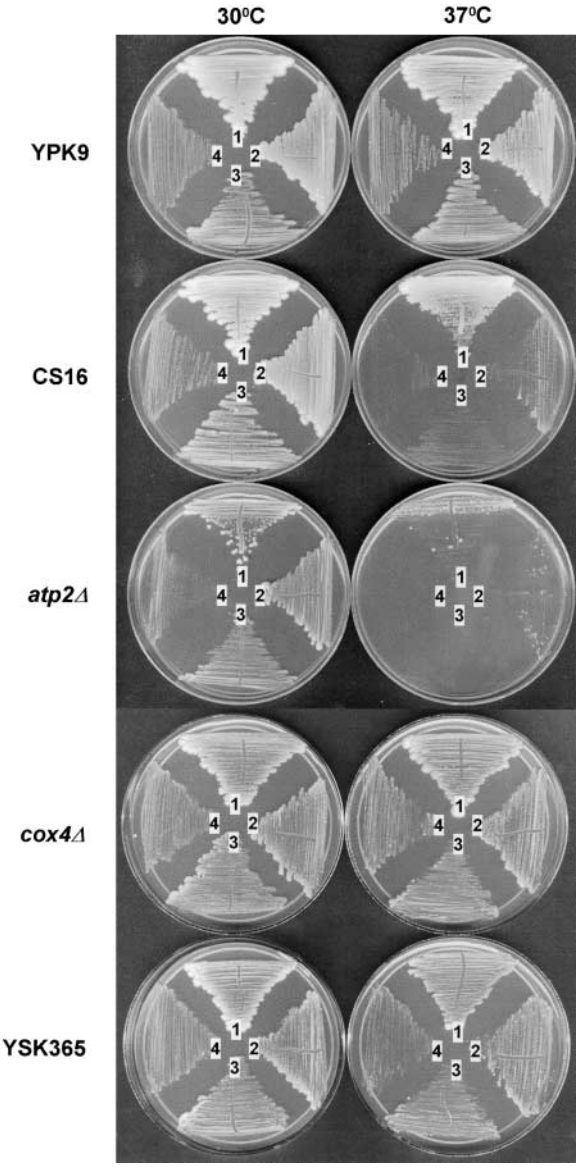

FIGURE 1.—Serial streaking of mutant CS16 and the parental wild-type strain YPK9. Plates were incubated at either 30° or 37°. After 48 hr of growth, cells from the first sector (1) were used to streak the second sector (2). The same procedure was repeated for the third (3) and fourth (4) sectors, except that cells were taken from the second and third sectors, respectively, after 48 hr of growth. For comparison, serial streaking was carried out with an *atp*2Δ strain, a *cox*4Δ strain, and a ρ^0 strain (YSK365).

RESULTS

Clonal senescence results from loss of age asymmetry in CS16: Clonal senescence mutants were isolated as described in MATERIALS AND METHODS, and one of them was chosen for further characterization. The mutant CS16 displayed clonal senescence at the restrictive temperature. Figure 1 shows the results of serial streaking

of the clonal-senescence mutant CS16 and the parental strain YPK9 at permissive and restrictive temperatures. CS16 growth was severely retarded by the third passage at 37°, while the wild type could be restreaked numerous times. At 30°, there was no evidence of clonal senescence on serial streaking for either CS16 or the parental strain YPK9.

Clonal senescence can result from a disruption of the age asymmetry between mother and daughter, such that daughters are not born with the potential for a full life span. It can also be caused by defects in the synthesis of essential cellular components or metabolites. The gradual dilution of these cellular ingredients through continuous cell divisions would eventually result in growth arrest of mothers and daughters equally. To distinguish between mutants of age asymmetry and such mutants of synthesis, a modified life-span determination experiment was performed. Virgin yeast cells produced at 30° were moved to 36° and allowed to divide seven times on average. The first six buds produced by these mother cells were removed and discarded by micromanipulation. The seventh buds and their mother cells were then moved back to 30°, and their remaining life spans at 30° were determined. In a mutant of synthesis, growth arrest results from disruption of specific synthetic activity. Upon temperature shift-down, the disrupted synthetic activity recovers and both mother and daughter cells resume normal growth. Since daughter cells are younger than mother cells, they should enjoy a longer mean life span than the mother cells' remaining life span (Figure 2A, bottom). Mutants of age asymmetry, on the other hand, produce daughter and mother cells of the same age at the restrictive temperature. Their ages remain the same, and thus they should have the same remaining life spans after the temperature shift-down (Figure 2A, top). Results from an experiment to distinguish mutants of age asymmetry from mutants of synthesis are shown in Figure 2, B and C. While wild-type daughter cells produced at 36° outlived their mother cells by more than four generations ($P < 0.00015$), those of the CS16 mutant had a mean life span statistically identical to the remaining life span of their mother cells ($P = 0.70$). Therefore, we conclude that CS16 is a mutant of age asymmetry.

Isolation of the gene mutated in CS16: Genetic analysis of the CS16 mutant showed that its clonal-senescence phenotype is the result of a single, semidominant mutation. A wild-type × CS16 heterozygous strain can grow indefinitely at 36° but produces smaller colonies than those of the corresponding wild type. We cloned the wild-type allele of CS16 by complementation for production of large colonies at restrictive temperature. We isolated 10 independent plasmid clones in this screen. All of these plasmids carried DNA inserts from the same region of yeast chromosome X. Deletion analysis narrowed the region to a single gene, *ATP2*.

Linkage analysis confirmed that *ATP2* is closely linked to the CS16 mutation. Strain CS16 was mated with a *MAT*α strain isogenic to YPK9, its parental strain. The resulting diploid strain was sporulated. The clonal-senescence phenotype segregated 2:2 in all tetrads analyzed. One of the *MAT*α segregants that displayed the clonal-senescence phenotype was isolated and designated CS16α. A *URA3* marker was inserted 400 bp downstream from the *ATP2* gene of YPK9, between this gene and the neighboring gene *CAF17*, by single-step insertion to produce strain YCL35. This strain was mated with CS16α. The diploid strain obtained this way was sporulated. Twenty tetrads were dissected and analyzed, and they all contained two Ura^- spores that showed the clonal-senescence phenotype at 36° and two Ura^+ spores that produced normal colonies at 36°.

A deletion of *ATP2* was generated in strain YPK9. The *atp2*Δ strains failed to grow on nonfermentable carbon sources such as glycerol, as expected. These strains also failed to grow under anaerobic conditions. However, on 2% glucose media, growth and cell morphology of these strains appeared normal at 30°. At 37°, the *atp2*Δ strains displayed the clonal-senescence phenotype similar to CS16 on serial streaking (Figure 1). However, the phenotype was more severe. The end-point colony sizes were usually smaller than that of CS16, and a dramatic reduction in the number of colonies occurred one or two sectors earlier. In contrast to the severe clonal-senescence phenotype of *atp2*Δ strains, other nuclear petites (*cox4*Δ), as well as mitochondrial petites (ρ^0), did not display any sign of clonal senescence (Figure 1).

Deletion of *ATP2* in strain W303-1A also resulted in a clonal-senescence phenotype, which manifested itself at 37°. Interestingly, however, this was observed only on YPR growth medium, in which glucose repression does not operate. This suggests that glucose derepression is a permissive factor for clonal senescence.

Identification of the *atp2* mutation in CS16: The *atp2* allele of CS16 was retrieved by plasmid gap repair. A total of 10 independent plasmids were isolated. These plasmids were purified from *E. coli*, introduced back into CS16, and tested for their ability to complement the clonal-senescence phenotype. Nine of these plasmids did not complement, suggesting that they carry the mutant allele. The *atp2* gene from 2 of these plasmids was sequenced (Figure 3A). In each case, only one identical base change was found. The G was replaced by an A at nucleotide 325, causing a valine-to-isoleucine substitution at the ninetieth amino acid of the mature polypeptide (amino acid 109 of the precursor). This valine is a very conserved residue, located in a conserved domain. Figure 3B shows sequences of the region adjacent to this residue from several species. Valine is present in most species. Except for the presence of alanine in a few species, no other amino acid has been found at this position. However, the function of this region remains obscure, because it has not been implicated in

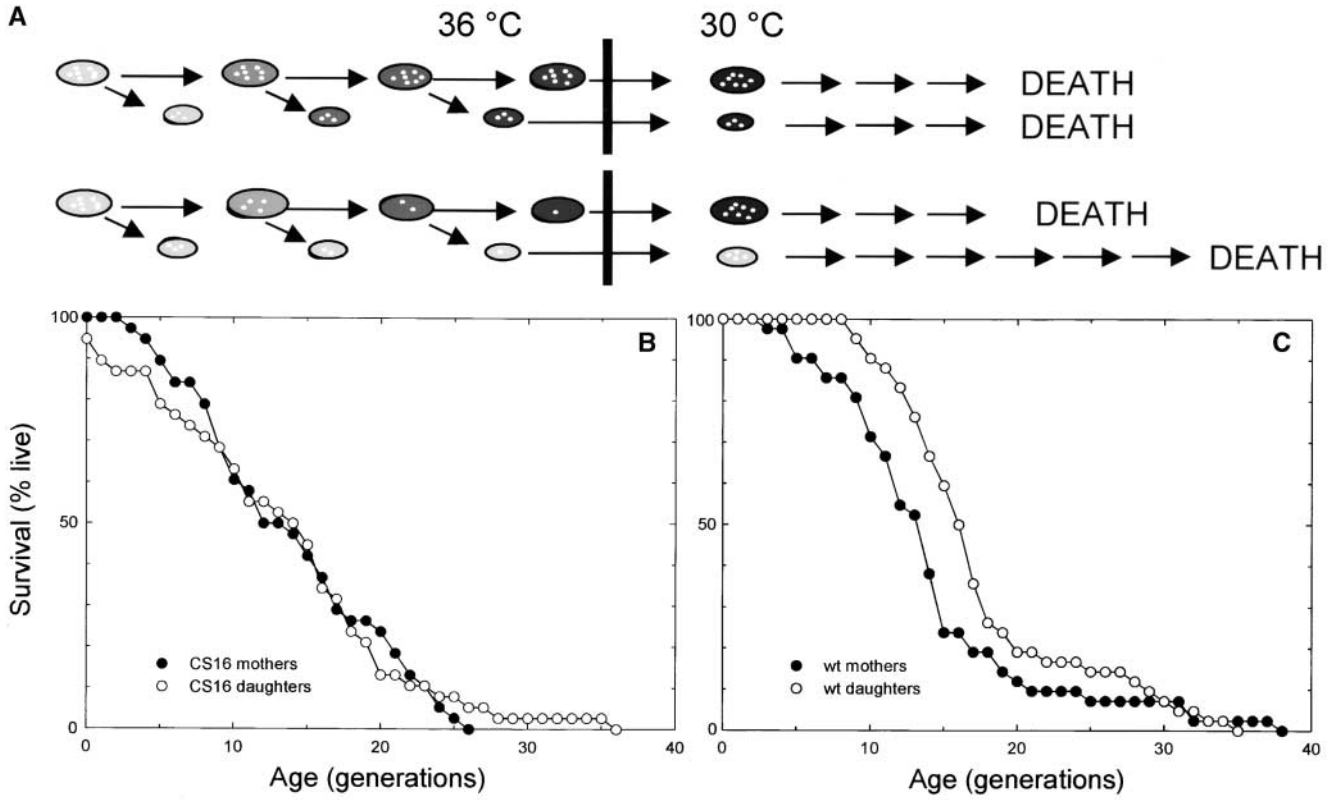

FIGURE 2.—CS16 is a mutant of age asymmetry. (A) In a mutant of age asymmetry (top), daughter cells have the same replicative age as their mothers when they are born, as depicted by their shade. Thus, a daughter produced at the restrictive temperature (36°) will have the same life span, measured in cell divisions, as that remaining to the mother, after lowering to permissive temperature (30°). In a mutant of synthesis (bottom), a vital substance (dots) is not made at restrictive temperature. The mother becomes older with each division (shading), but daughters are born young. Thus, the daughters have a longer remaining life span than that of their mothers after the cells are returned to permissive temperature, because the synthesis of the vital substance resumes. (B) CS16 mother cells were kept at 36°. The first six daughters of each mother were removed. The life spans of the seventh daughters and the remaining life spans of their mothers were subsequently determined at 30°. The mean life span of the daughters was 13.3 generations, while that remaining to their mothers was 13.9 generations ($P = 0.70$). (C) The experiment described in B for CS16 was carried out in parallel for the wild-type parental strain YPK9. The mean life span of the daughters (17.7 generations) was longer ($P < 0.00015$) than the mean remaining life span of the mothers (13.2 generations).

nucleotide binding or enzyme activity (ABRAHAMS *et al.* 1994; SHEN *et al.* 1996; BAKHTIARI *et al.* 1999).

Growth characteristics of CS16 cultures: *ATP2* belongs to the class of mitochondrial genome integrity genes, which affect mitochondrial DNA stability (CHEN and CLARK-WALKER 1996). However, only specific point mutations altering Arg435 elicit this phenotype. Atp2p is the β-subunit of F_1-ATPase, which contributes to the catalytic activity of the ATP synthase and is coupled to the respiratory chain in the inner mitochondrial membrane (BOYER 1997). The β-subunit not only is involved in the self-assembly of the ATPase, but it also plays a role in the assembly of other components of the respiratory chain, such as cytochrome oxidase (ASCHENBRENNER *et al.* 1993; LIANG and ACKERMAN 1996; LAI-ZHANG *et al.* 1999). One might expect that the CS16 mutant would exhibit a growth defect on nonfermentable carbon sources or show an increase in the frequency of spontaneous petites on fermentable carbon sources (petite positive).

We compared the growth rates of CS16 and its parental strain YPK9 at 30° on YPD (glucose) and found them to be indistinguishable (112-min doubling time). There was also no significant difference between the two strains grown on YPG (glycerol) at either 30° (173 and 156 min for YPK9 and CS16, respectively) or 37° (216 and 218 min, respectively), although growth was slower at the elevated temperature. Combination of CS16 with a ρ^- background markedly diminished growth rate (285-min doubling time) compared to a ρ^- YPK9 (146-min doubling time) on YPD at 30°.

The CS16 mutant did not appear to accumulate petites excessively at either 30° or 37°, as compared to YPK9 (Figure 4). Indeed, the frequency of petites in CS16 cultures is much lower and begins to equal that found in YPK9 only upon prolonged culture at 37°. However, the viability of CS16 declined at 37°, becoming significantly lower than that of its parental strain YPK9 after 48 hr. This loss of viability was associated with clonal senescence (Figure 1). The temperature sensitiv-

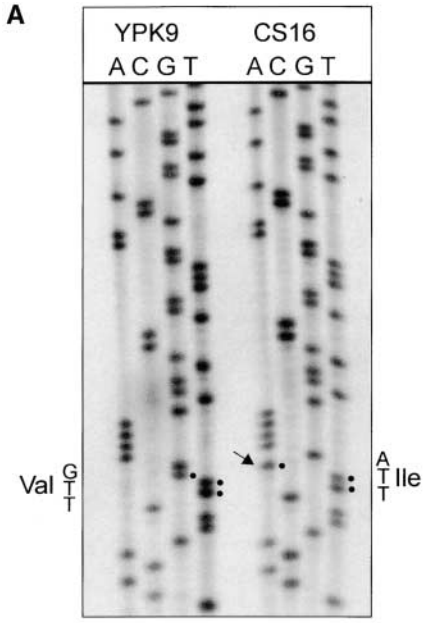

B

tvrtiamdgteglvrgek**v**ldtggpisvpv	*S. cerevisiae*
tvrtiamdgteglvrgen**v**sdtgapisvpv	*K. lactis*
tvrtiamdgteglvrgta**v**idtgspisipv	*S. pombe*
vvrciamdgteglvrgak**a**sdtgapitipv	*N. crassa*
tvrtiamdgteglvrgqk**v**ldsgapikipv	*H. sapiens*
tvrtiamdgteglvrgqk**v**ldtgypiripv	*D. melanogaster*
vvrciamdgteglvrgqp**v**adtgdpikipv	*C. elegans*
mvrtiamdgteglvrgqr**v**lntgspitvpv	*Z. mays*
ivrtiamgssdglrrgld**v**kdlehpievpv	*E. coli*
tvrtiamastdgvqrgme**a**vdtgapisvpv	*B. subtilis*
kvravamsatdgltrgmr**v**idtgaplsvpv	*P. abies* (chloroplast)

FIGURE 3.—Identification of the CS16 mutation in *atp2*. (A) The CS16 mutant was isolated by plasmid gap repair and the DNA was sequenced alongside the wild-type allele. A portion of the sequencing autoradiogram is presented. The mutated base is indicated by an arrow, and the consequence for protein coding is shown. (B) The amino acid sequences of the affected region in the β-subunits of F_1-ATPase from *S. cerevisiae*, *Kluyveromyces lactis*, *Schizosaccharomyces pombe*, *Neurospora crassa*, *Homo sapiens*, *Drosophila melanogaster*, *Caenorhabditis elegans*, *Zea mays*, *E. coli*, *Bacillus subtilis*, and *Picea abies* are shown for comparison. The site corresponding to the mutation in CS16 is indicated by boldface type.

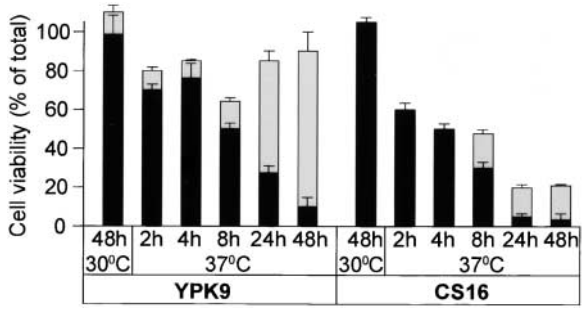

FIGURE 4.—Loss of viability and accumulation of petites during clonal senescence. CS16 and its wild-type parental strain YPK9 were grown at 30° or 37° in YPD. Samples were withdrawn at various times, and cells were counted in a hemacytometer and plated on both YPD and YPG to determine the fraction of viable cells and the content of petites. (Petites lack fully functional mitochondria and cannot grow on YPG.) Each bar indicates the total cell viability, while the shaded and solid portions denote the fraction of petites and grandes, respectively. The error bars designate the SE.

ity of the clonal-senescence phenotype in the CS16 point mutant is apparently not due to a temperature-sensitive mutation in the F_1-ATPase itself, because *atp2*Δ mutants also show thermo-sensitive clonal senescence.

Telomere attrition and ERC accumulation are not the cause of clonal senescence in *atp2* mutants: It is known that induction of telomere shortening leads to the extinction of yeast clones similar to a senescent phenotype (LUNDBLAD and SZOSTAK 1989). However, there is no evidence that this involves a loss of age asymmetry between mother and daughter cells. We explored the possibility that the proximal cause of the clonal-senescence phenotype associated with the loss of age asymmetry in CS16 and the *atp2*Δ strain could be telomere attrition (Figure 5A). There was no evidence for a change in the electrophoretic mobility of the terminal restriction fragments of XY′ telomeres at restrictive temperature, even after four serial streakings. Clonal senescence had resulted in a dramatic reduction in cell viability in these strains at this time, as compared to the wild-type parent (Figures 1 and 4).

It has been shown that the accumulation of ERCs, a process that usually occurs during the yeast replicative life span, can kill yeast (SINCLAIR *et al.* 1998). Although pedigree analyses indicate that ERCs are not likely to cause clonal senescence because they rarely are transmitted to the daughters of young mothers, we examined the possibility that ERC accumulation may be the proximal cause of clonal senescence in CS16 and the *atp2*Δ strain. There was little, if any, change in the intracellular ERC content of cells, even after clonal senescence was very pronounced (Figure 5D). Thus, ERC accumulation is not the cause of clonal senescence.

Effect of mutation in *ATP2* on mitochondrial membrane potential (ΔΨ): Yeast cells grown on nonfermentable carbon sources derive energy primarily through the synthesis of ATP by ATP synthase, which is driven by the activity of the electron transport chain (GANCEDO and SERRANO 1989). The electron transport chain, under these conditions, generates the ΔΨ that provides energy for the transport of metabolites across the inner mitochondrial membrane. In the absence of a functional respiratory chain, cells reverse the activity of ATP synthase, using ATP to establish ΔΨ (BUCHET and GODINOT 1998). When grown on a fermentable carbon source, yeast derive the bulk of their energy through the glycolytic pathway by fermentation. In this case, the synthesized ATP is utilized by the ATPase activity of ATP synthase to generate the requisite ΔΨ. Yeast may also establish ΔΨ by a third mechanism involving the ADP/

ATP translocator (DUPONT *et al.* 1985). The expression of the clonal-senescence phenotype of CS16 on glucose rather than on glycerol suggested the possibility that the mutation in *ATP2* might affect $\Delta\Psi$.

We examined the $\Delta\Psi$ of CS16 cells undergoing progressive clonal senescence by flow cytometry (Figure 6, A–D). At 37°, there was a shift of the cell population to higher $\Delta\Psi$ values for both CS16 and the YPK9 control, as visualized by the JC-1 stain. However, a new population of CS16 cells with a low $\Delta\Psi$ appeared at this temperature, and this population progressively increased in number as clonal senescence became more and more extensive. The shift to higher $\Delta\Psi$ values coincided with an increase in mitochondrial mass, as evidenced by NAO staining (Figure 6, E–H). The population of CS16 cells exhibiting low $\Delta\Psi$ was associated with a decline in mitochondrial mass. However, this loss of mitochondrial mass was delayed compared to the loss of $\Delta\Psi$. The rates of decline of $\Delta\Psi$ and mitochondrial mass are quantified in Figure 6, I and J. Double staining with JC-1 and Calcofluor revealed that the population of CS16 cells with low $\Delta\Psi$ contained primarily young cells with few or no bud scars (Figure 6, K and L). It is possible to estimate the extent of mitochondrial depletion in CS16 at 37° from the flow cytometry following NAO staining. There was an average decrease in mitochondrial mass of ~40-fold (Figure 6H) in 50% of the cells (Figure 6J).

Morphology and segregation of mitochondria in the *atp2* mutant: The collapse of $\Delta\Psi$ and loss of mitochondria in CS16 indicated by the flow-cytometric analysis prompted us to examine mitochondria in these cells by microscopy. The morphology and distribution of mitochondria in the cells was visualized in a confocal microscope after staining for the outer membrane protein porin. Mitochondria in CS16 at 30° and YPK9 at 30° and 37° (Figure 7) displayed the normal tubular morphology and permeated the entire cell volume. In CS16 at 37° (Figure 7), the mitochondria appeared punctate and tended to form one or a few large aggregates with progressive clonal senescence.

The results obtained with the confocal microscope were confirmed by fluorescence microscopy (Figure 8). We found, furthermore, that unlike the wild-type, parental strain YPK9 incubated at 37°, CS16 undergoing clonal senescence at 37° frequently segregated few or no mitochondria to daughters (buds). As clonal senescence progressed (Figure 8, 37° for 48 hr), many of the CS16

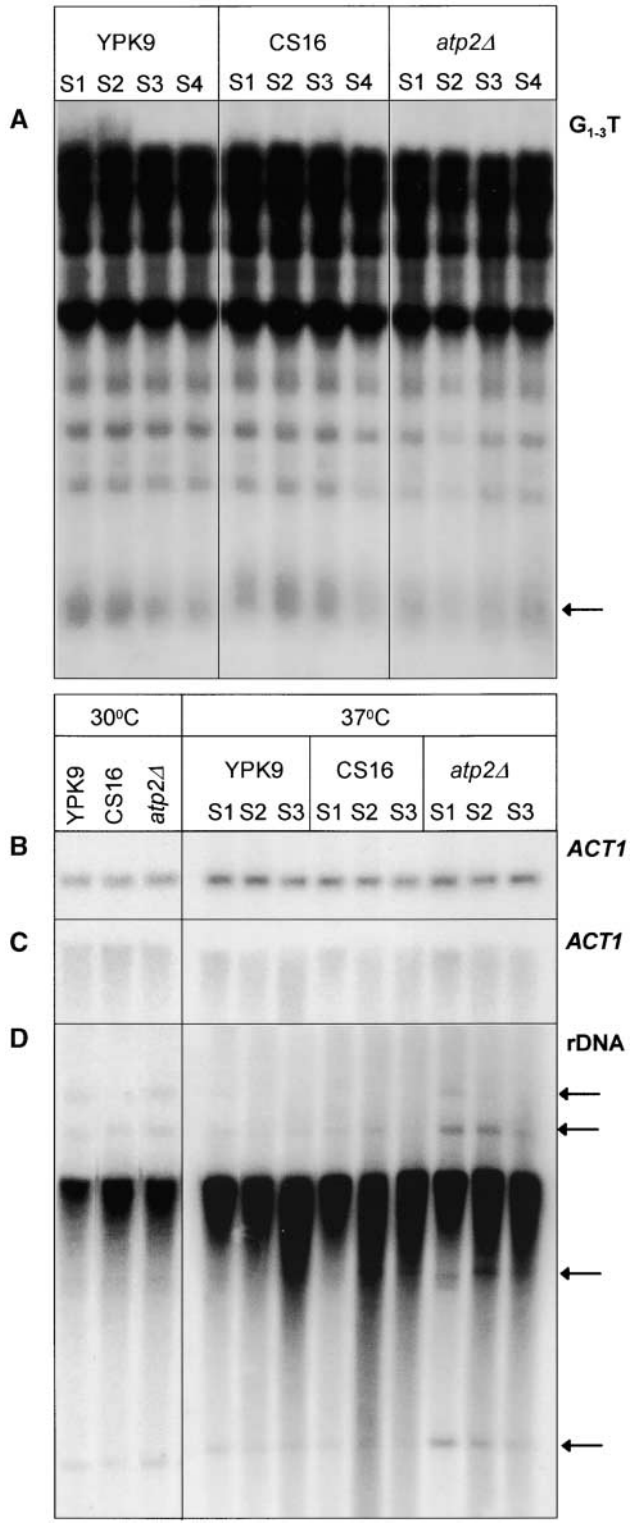

FIGURE 5.—Clonal senescence is not the result of telomere shortening or accumulation of ERCs. (A) YPK9 (wild-type parental strain), CS16 mutant, and the *atp2*Δ strains were serially streaked as in Figure 1 at 37°. Cells from the first through the fourth sectors (S1–S4) were scraped from plates, washed with deionized water, and used for isolation of genomic DNA. In a Southern blot, the terminal restriction fragment (arrow) containing the yeast telomeres was detected as described in MATERIALS AND METHODS. (B) Cells were collected as in A above, with cells plated at 30° for comparison. The DNA was digested with *Spe*I, blotted as described in MATERIALS AND METHODS, and hybridized with the *ACT1* probe to confirm equal loading of the gel. (C) The same amount of undigested DNA was separated and also probed with *ACT1*. (D) The same blot as in C was subsequently hybridized with an rDNA probe. The arrows point to the unit rDNA repeat-containing ERC (bottom arrow) and its higher concatamers.

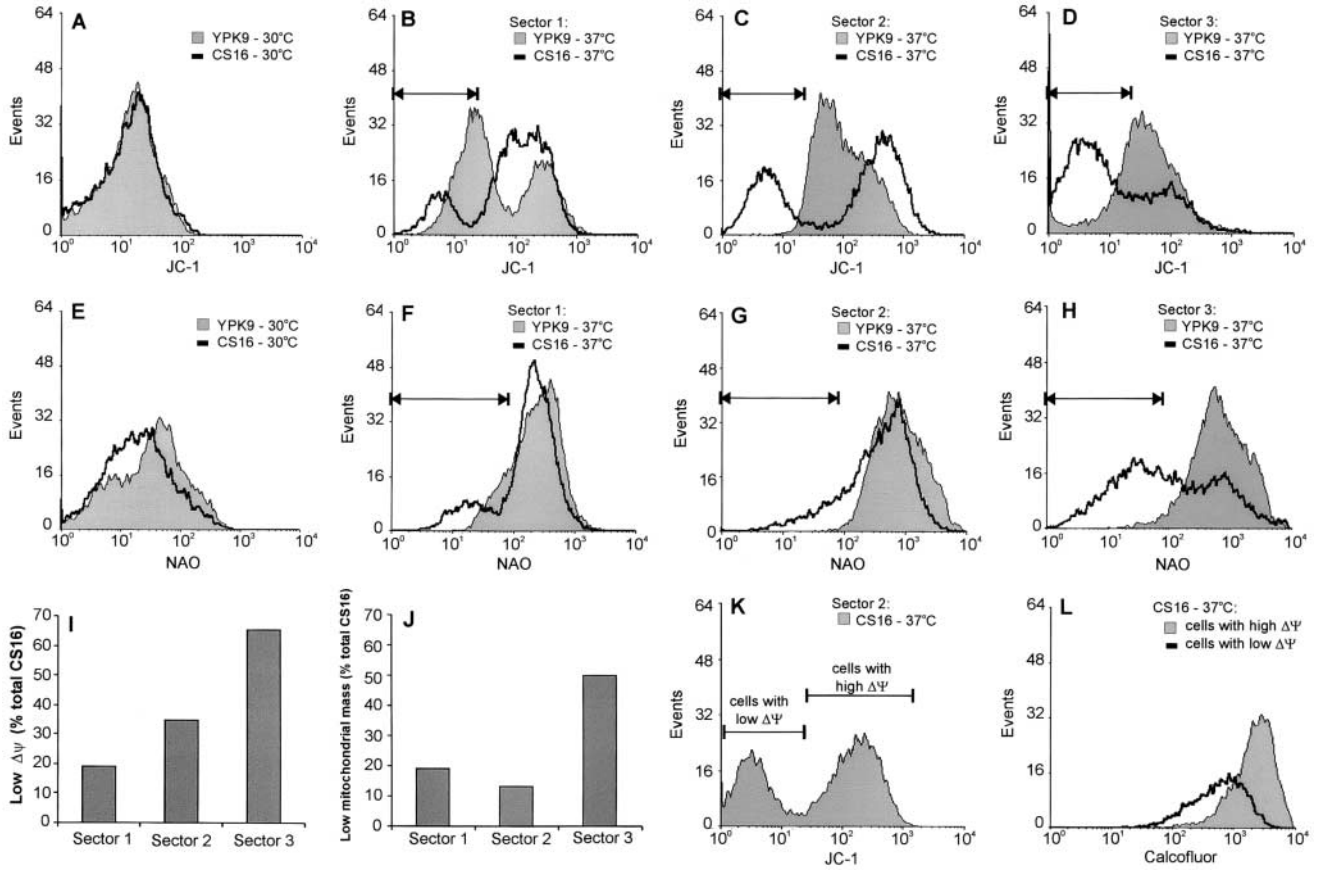

FIGURE 6.—Loss of mitochondrial membrane potential (ΔΨ) during clonal senescence. YPK9 (wild-type parental strain) and CS16 cells were subjected to serial streaking at 37° as in Figure 1. Cells from the first through third sectors are shown in B–D and F–H. For comparison, cells were plated at 30° (A and E). Cells were scraped from plates, suspended in YPD medium, and stained with JC-1 for ΔΨ (A–D) or NAO for mitochondrial mass (E–H) and analyzed by flow cytometry, as described in MATERIALS AND METHODS. The fraction of the cells of low ΔΨ and of low mitochondrial mass is indicated by the arrows and plotted in I and J, respectively. CS16 cells from sector 2 of the serial streaking plate were stained with both JC-1 and Calcofluor to quantify bud scars, as described in MATERIALS AND METHODS. The cells of low and high ΔΨ (K), indicated by the bracketed lines, were analyzed for bud scars (L). The number of events (cells) are plotted as a function of fluorescence intensity for a total of 10,000 cells in A–L. In a control, JC-1-stained cells were treated with carbonyl cyanide *p*-trifluoromethoxyphenylhydrazone (FCCP) to collapse the ΔΨ for verification of the specificity of the stain (not shown).

cells became devoid of mitochondria, as determined by staining for porin. This result was confirmed by staining with NAO for mitochondrial membrane and 4′,6-diamidino-2-phenylindole for mitochondrial DNA (not shown).

To further examine the series of events in CS16, functional mitochondria were visualized in viable cells by staining with Mitotracker Red, which requires membrane potential for uptake (Figure 9). As with porin staining, a defect in segregation of active mitochondria to buds was apparent, as was a progressive loss of visible mitochondria in general, with increasing clonal senescence (Figure 9, D and F). However, these cellular deficits in functional mitochondria preceded the same events as observed by porin staining for mitochondrial mass (Figure 8). These results are consistent with those obtained by flow cytometry, which showed that a collapse in ΔΨ precedes the loss of mitochondrial mass (Figure 6).

Effect of aging on mitochondria: The loss of ΔΨ appears to result in the lack of proper segregation of mitochondria, followed by mitochondrial loss leading to clonal senescence. Could this train of events be involved in normal yeast aging? We examined ΔΨ as a function of replicative age by flow cytometry after staining with JC-1 and Calcofluor (Figure 10). Clearly, there was an increase in ΔΨ as a function of age, as depicted by the linear approximation of the dependence of ΔΨ on bud scar number. However, there was an even greater increase in mitochondrial mass with age, as evidenced by staining with NAO and Calcofluor. This increase was about fivefold greater than the increase in ΔΨ, as judged by the slopes of the linear approximations. This indicates a fivefold decline in ΔΨ with replicative age. Thus, mitochondrial dysfunction accumulates during the replicative life span.

Young and old yeast cells were prepared by fluorescence-activated cell sorting after staining with Cal-

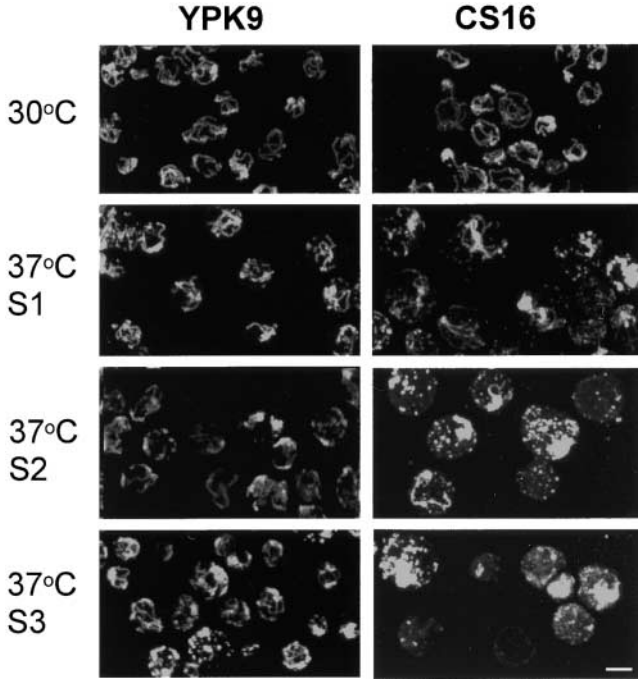

FIGURE 7.—Morphology and distribution of mitochondria in CS16 cells. Cells were plated on YPD at 30° or serially streaked at 37° as in Figure 1 and collected from the first (S1), second (S2), and third (S3) sectors. The cells were stained with antiporin antibody and examined by confocal fluorescence microscopy to visualize mitochondria, as described in MATERIALS AND METHODS. Bar, 10 μm.

cofluor. We determined the propensity of the sorted cells to produce daughters with low $\Delta\Psi$. Older cells had a tendency to have daughters with low relative $\Delta\Psi$ (Figure 11C), as a consequence of segregating mitochondria deficient in $\Delta\Psi$ (Figure 11B) rather than as a consequence of a difference in mitochondrial mass partitioned (Figure 11A). Thus, events similar to those induced in *atp2* mutants that result in loss of age asymmetry and clonal senescence also occur as a consequence of normal replicative aging in yeast.

DISCUSSION

We have developed an isolation scheme for age-asymmetry mutants in yeast that display clonal senescence (Figure 1). Two distinct mutants were isolated, one of which has been characterized in detail. This mutant, CS16, has a point mutation in the *ATP2* gene (Figure 3), which encodes the β-subunit of the mitochondrial F_1-ATPase. This mutation disrupts the age asymmetry between mother and daughter yeast cells (Figure 2). Similar, although more drastic, effects are observed in an *atp2*Δ strain (Figure 1). The CS16 mutant is indistinguishable from the wild-type YPK9 in its growth rate on both fermentable and nonfermentable carbon sources. Elimination of mitochondrial DNA was needed in conjunction with CS16 (or *atp2*Δ) to reduce growth rate, and it did so drastically. CS16 did not accumulate petites in comparison with YPK9. However, it suffered a progressive and extensive loss of viability on both solid and liquid media at the restrictive temperature (Figure 4), which was associated with clonal senescence (Figure 1). This loss of viability appeared to result from a loss of mitochondrial mass and not simply from a loss of mitochondrial function (Figures 6, 8, and 9). The expression of the clonal-senescence phenotype was under glucose repression.

Mutations in *ATP2* do not induce telomere attrition nor do they result in the accumulation of ERCs to cause clonal senescence (Figure 5). However, they do lead to the loss of $\Delta\Psi$, which precedes the loss of mitochondrial mass during clonal senescence (Figures 6, 8, and 9). The cells that have lost mitochondria are primarily young cells. The loss of $\Delta\Psi$ coincides with changes in the morphology and intracellular distribution of mitochondria (Figure 7), and this is accompanied by lack of segregation of normal numbers of mitochondria to daughter cells (Figures 8 and 9). The loss of $\Delta\Psi$ found in clonal senescence also occurs as a consequence of normal aging in yeast (Figure 10), and old yeast have a tendency to segregate inactive mitochondria to their daughters (Figure 11).

Our results indicate that proper segregation of mitochondria is important in the establishment of age asymmetry between mothers and daughters. They also implicate $\Delta\Psi$ in this process. The clonal senescence induced by mutations in *ATP2* appears to result from the mitochondrial dysfunction that they precipitate. Similar mitochondrial dysfunction and loss of age asymmetry occurs normally during yeast aging. We propose the following model to explain these findings (Figure 12). Mitochondrial dysfunction increases with age in yeast, as it does in mammalian cells (ARNHEIM and CORTOPASSI 1992). Thus, old yeasts tend to segregate dysfunctional mitochondria to their daughters, leading to a lower replicative potential on their part. Indeed, the daughters of old yeast cells generally have a lower replicative potential than that of the daughters of young cells (JAZWINSKI 1993; KENNEDY *et al.* 1994). The source of mitochondrial dysfunction in old yeast cells may be oxidative stress (LAUN *et al.* 2001). In CS16, these effects are exacerbated, leading to the loss of age asymmetry with a lower replicative potential for daughters and the development of clonal senescence.

Clonal senescence mutants have been isolated previously. The induction of telomere shortening leads to clonal senescence in yeast (LUNDBLAD and SZOSTAK 1989). However, this is not the result of a loss of age asymmetry. Telomeres do not normally shorten during yeast aging (D'MELLO and JAZWINSKI 1991).

By comparing the generation times of daughter cells produced by mother cells of different ages, EGILMEZ and JAZWINSKI (1989) provided evidence for a cytoplasmic senescence factor. The accumulation of this factor ap-

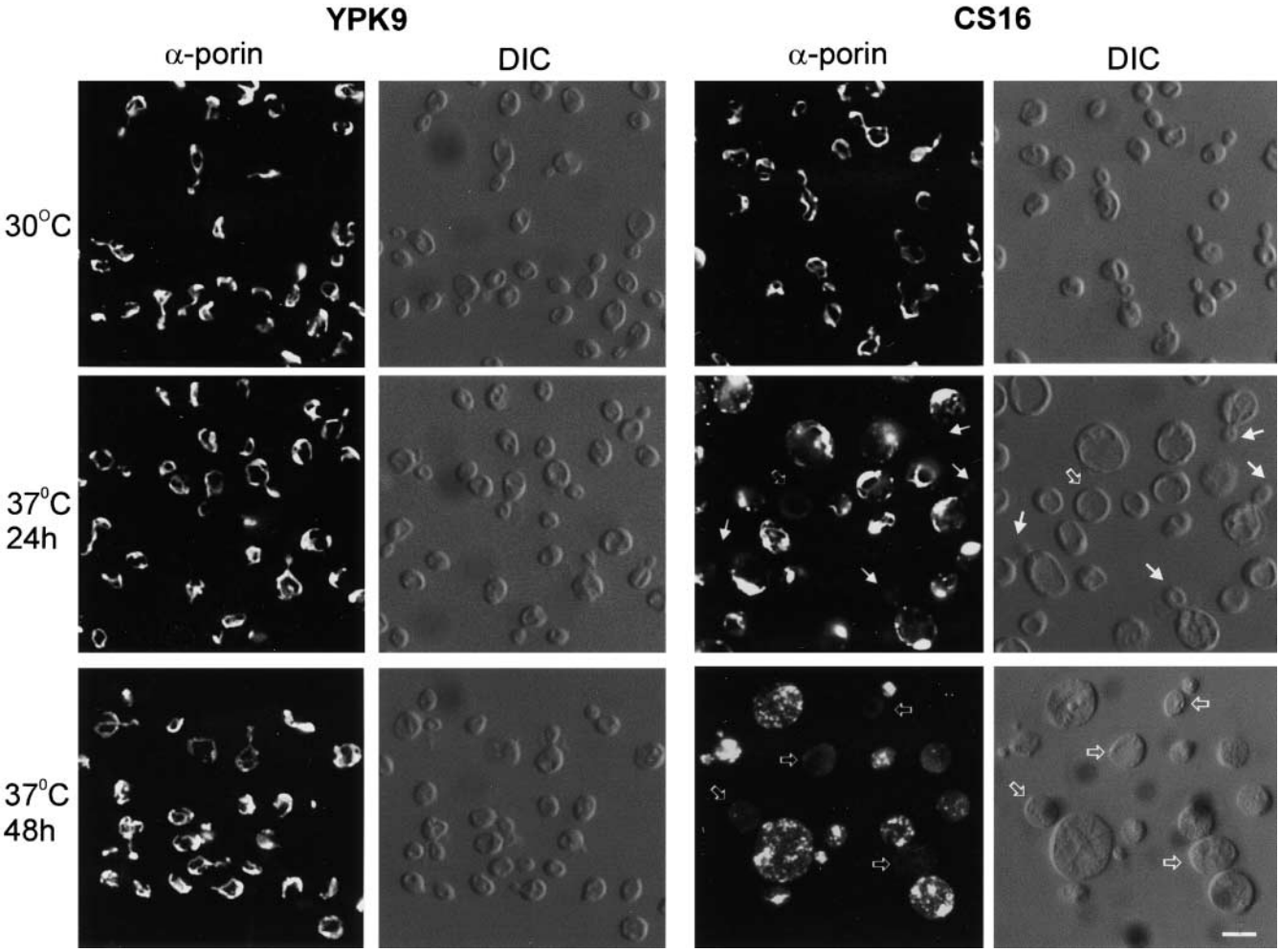

Figure 8.—Segregation of mitochondria in CS16 cells. YPK9 (wild-type parental strain) and CS16 cells were grown in YPD at 30° for 24 hr or at 37° for 24 or 48 hr. Mitochondria were visualized using an antiporin antibody and a fluorescent secondary antibody, as described in materials and methods. The cells in the same microscope fields were observed using Nomarski differential interference contrast (DIC). Cells (open arrows) and buds (solid arrows) with few or no mitochondria are indicated. Bar, 10 μm.

pears to be responsible for at least some senescence phenotypes in yeast, such as prolonged generation time. The authors suggested that this factor is produced and accumulated in aged mother cells, but can be relatively quickly disposed of by young daughter cells. Such a mechanism implies the dependence of age asymmetry upon the ability of young cells to remove the senescence factor. Indeed, if the senescence factor is dysfunctional mitochondria, they may be replenished and/or repaired in daughter cells, provided their amount is not overwhelming.

Sinclair *et al.* (1998) discovered that ERCs are a cause of aging in yeast. ERCs appear to have many of the features of a senescence factor. The amount of ERCs in yeast cells increases with age. Accumulation of an artificial ERC reduces the replicative capacity of yeast cells. Pedigree analysis showed that ERCs segregrate preferentially to mother cells during cell division. However, they do not cause clonal senescence, even when their accumulation is markedly enhanced (Sinclair *et al.* 1998). In fact, increased ERC levels are associated with longer replicative life spans under certain circumstances (Conrad-Webb and Butow 1995; Kirchman *et al.* 1999).

The evolutionary theory of aging has pointed out that aging has multiple causes. Therefore, the establishment of age asymmetry is also likely to depend upon numerous mechanisms and structures. A logical step in identifying elements essential for age asymmetry is to isolate mutants with defects in maintenance of age asymmetry. We initiated a genetic screen for age-asymmetry mutants by looking for strains that display a clonal-senescence phenotype. We anticipated a requirement for "filtering" of damaged constituents from daughter cells as essential for establishment of heritable age asymmetry (Egilmez and Jazwinski 1989). Surprisingly, CS16, the first age-asymmetry mutant we isolated, was in *ATP2*. CS16 does not simply display a defect in mitochondrial inheri-

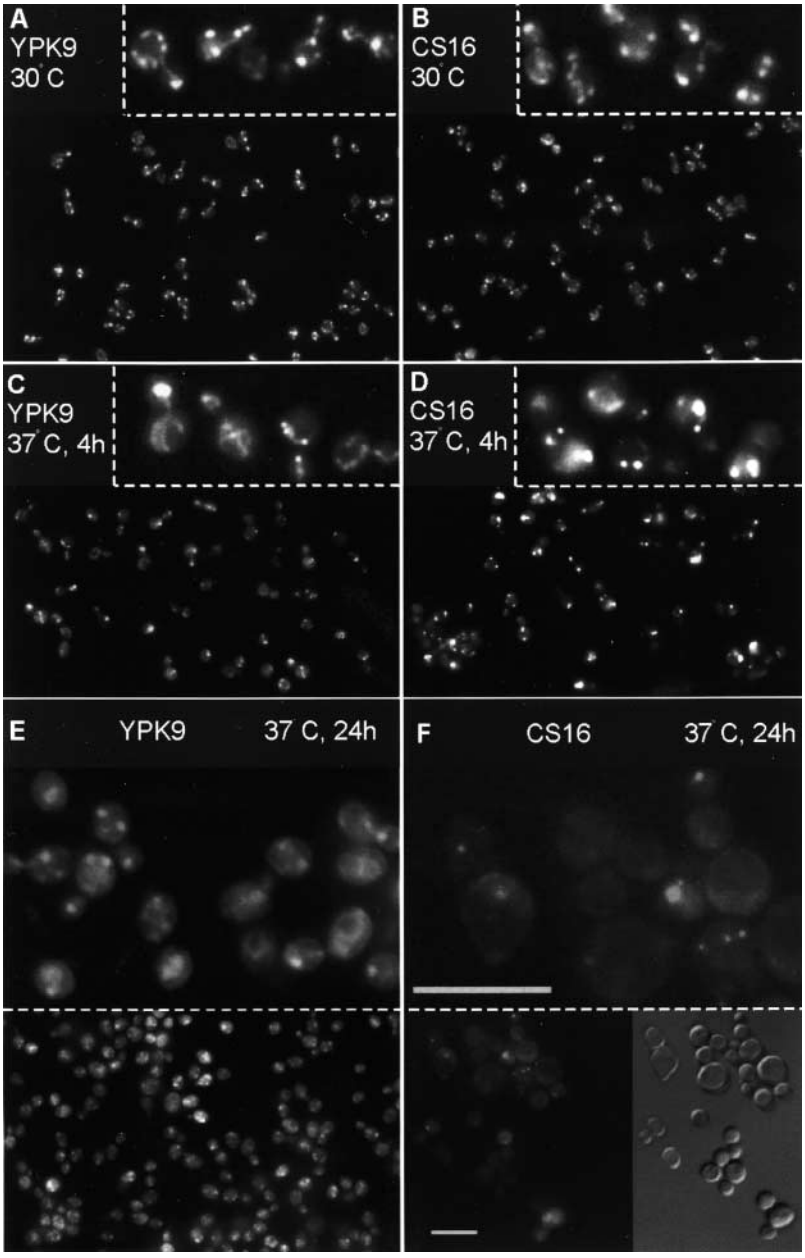

FIGURE 9.—Loss of functional mitochondria in CS16 cells. YPK9 (wild-type parental strain; A, C, and E) and CS16 (B, D, and F) cells were grown in YPD containing 120 μg/ml adenine for 24 hr at 30° (A and B) or at 37° for 4 hr (C and D) or 24 hr (E and F). Cells grew exponentially. They were stained with Mitotracker Red and examined by fluorescence microscopy to visualize mitochondria, as described in MATERIALS AND METHODS. The insets in A–F show cells at higher magnification. The bottom right section of F shows the field on the left using DIC. Bar, 20 μm.

tance. Instead, it causes a mother cell to produce daughters that reflect its own age (Figure 2), suggesting that they inherit a "senescence factor." This senescence factor may be a paucity of fully functional mitochondria or the presence of damaged mitochondria from which the daughter cannot readily recover. Thus, the effects of CS16 are subtle and delayed both within a cell lineage and within an individual dividing cell, unlike the immediate consequences of the mutants of mitochondrial inheritance that have been isolated by others (YAFFE 1999). These latter mutants do not display clonal senescence, a process that plays itself out over many cell generations.

Mother-daughter asymmetry has been the subject of analysis in yeast, since STRATHERN and HERSKOWITZ (1979) found that only mothers can switch mating type. A detailed molecular description of this phenomenon has been emerging, and it is clear that this difference in cell fates depends on the localization of *ASH1* mRNA to buds (SIL and HERSKOWITZ 1996). In this case, a developmental decision is made at each cell division, but there is no evidence that the process or the effect on the daughter changes depending on the replicative age of the mother cell. However, it is possible to imagine that the kind of age asymmetry described in our report and the resulting clonal senescence could result from perturbations in the machinery involved in the mating-type switch process. Similarly, mutations in bud formation, cell polarity, or organelle movement and inheritance could lead to loss of age asymmetry.

The primary function of F_1, F_0-ATPase in yeast is ATP synthesis. However, our results suggest that this enzyme

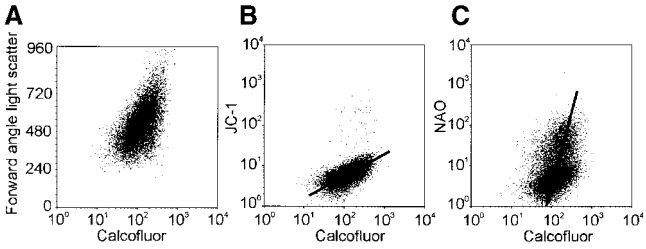

FIGURE 10.—Loss of ΔΨ as cells age. Exponentially growing YPK9 cells in YPD at 30° were stained with either JC-1 or NAO followed by Calcofluor, or with Calcofluor alone, and analyzed by flow cytometry, as described in MATERIALS AND METHODS. (A) Forward-angle light scatter (measure of cell size), (B) JC-1 fluorescence, and (C) NAO fluorescence, as a function of Calcofluor fluorescence. A total of 10,000 cells were analyzed in each case. The heavy solid lines in B and C are the linear approximations of the cell distributions.

is also involved in establishing age asymmetry. The F_1, F_0-ATPase clearly has functions independent of the ATP-synthesizing activity. One of these functions is required for optimal growth of ρ^- cells or ρ^+ cells under anaerobic conditions, where oxidative phosphorylation does not take place. The role of F_1, F_0-ATPase in these conditions is possibly maintenance of a proper ΔΨ. In human cells, ΔΨ can be maintained by a functioning electron transport chain, the ATP-dependent proton pumping activity of F_1, F_0-ATPase, or the electrogenic ADP/ATP exchange activity of mitochondrial ADP/ATP translocator enzymes (BUCHET and GODINOT 1998). It is likely that all three mechanisms function in yeast as well (DUPONT *et al.* 1985). The marked reduction in steady-state frequency of petites in CS16 compared to wild type (Figure 4) can be explained by the selective disadvantage they possess, due to compromise in the ability of F_1-ATPase to hydrolyze ATP and thus to cooperate with the electrogenic activity of the ADP/ATP translocator. Interestingly, in the ADP/ATP translocator mutant *op1*, loss of mitochondrial DNA results in a limited growth phenotype showing some similarity to the clonal-senescence phenotype of CS16 (Kováčová *et al.* 1968; KOLAROV *et al.* 1990). The slow growth rates of petite strains derived from CS16 suggest a possible deficit in ATP hydrolysis by F_1-ATPase that leads to reduced electrogenic activity of the ADP/ATP translocator in CS16 and combines with the lack of proton pumping by F_1, F_0-ATPase in the petite, which becomes evident when the electron transport chain is not functional. Clearly, the elimination of electron transport-generated ΔΨ (*cox4*Δ) or electron transport and F_1, F_0-ATPase proton pumping (ρ^0) does not result in clonal senescence (Figure 1). The clonal-senescence phenotype is observed only on fermentable carbon sources, a condition in which the electron transport chain is not very active (GANCEDO and SERRANO 1989). Under such conditions, the cell would be largely dependent on the F_1, F_0-ATPase to generate ΔΨ, a function that may be suboptimal in

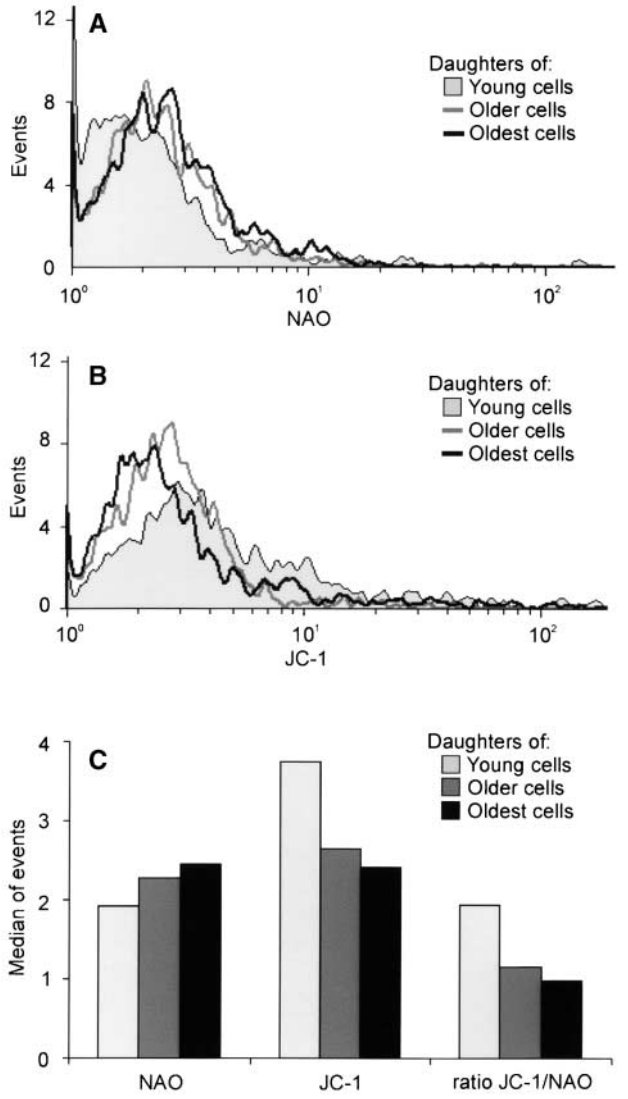

FIGURE 11.—Older cells produce daughters with low ΔΨ. YPK9 cells were grown on YPD at 30° in exponential phase, collected, and stained with Calcofluor, as described in MATERIALS AND METHODS. They were separated into three fractions containing cells of different replicative ages by fluorescence-activated cell sorting (7500 cells/sec), according to Calcofluor fluorescence and cell size as in Figure 10A (KIM *et al.* 1996). These fractions (2.5×10^5 cells) were returned to culture for 2.5 hr, after which most of the cells budded, but no more than once. The cells were restained with Calcofluor and analyzed by flow cytometry to determine the mitochondrial mass (A) and ΔΨ (B) of the daughter cells by NAO and JC-1 staining as before. The smallest 10% of the restained cells, which showed background Calcofluor fluorescence, were analyzed in this manner. The analysis of 1000 cells each is shown in A and B. The median of events (cell distributions) for the NAO and the JC-1 staining, as well as for the JC-1/NAO ratio is shown in C.

CS16. Perhaps the ADP/ATP translocator also cannot suffice without a fully active F_1-ATPase. It will be interesting to determine whether mutations in the translocator are synthetic to *atp2*.

The delayed effects of CS16 or *atp2*Δ may be ex-

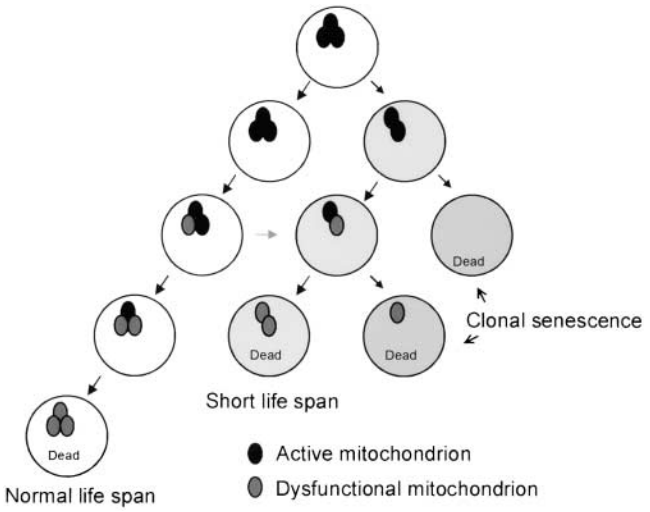

FIGURE 12.—Model depicting the consequences of the loss of age asymmetry. Wild-type cells have a life span of normal length. Cell death may be caused, among other reasons, by the accumulation of dysfunctional mitochondria. In a mutant of age asymmetry or when age asymmetry is compromised in other ways, daughters are produced that do not receive a full complement of active mitochondria, which accelerates the loss of functional mitochondria and shortens life span. Older mothers of such mutants would produce daughters (shaded, horizontal arrow) that not only may have fewer mitochondria but also have less functional mitochondria. Repeated growth of age-asymmetry mutant cells results in the enrichment of daughter cells that lack functional mitochondria or lack mitochondria entirely.

plained by postulating the gradual accumulation of cellular damage, in particular to mitochondria, which exhibit progressive functional decline manifested in loss of $\Delta\Psi$. These events could play out at the molecular level in several ways. Atp2p is important not only for assembly of the ATP synthase itself but also for assembly of protein complexes of the electron transport chain, as indicated earlier. Thus, alterations in Atp2p could disrupt mitochondrial stability. In similar fashion, Atp2p might affect the assembly of the protein complexes that are involved in mitochondrial distribution and inheritance, either directly or through $\Delta\Psi$. These are only examples of the possibilities.

The studies we have described may have implications for human aging. Mitochondrial dysfunction is associated with aging in humans (WALLACE 1999). At a more fundamental level, the mechanisms underlying the maintenance of age asymmetry within stem cell lineages have significant ramifications not only for aging but for other human disorders as well. The yeast model provides a useful tool for the dissection of these mechanisms.

The skillful help of Luis Marrero with confocal microscopy and Phil Constantin with fluorescence microscopy is greatly appreciated. This work was supported by grants from the National Institute on Aging of the National Institutes of Health (U.S.P.H.S.) and by a gift from Heinz Keller of Tasmania.

LITERATURE CITED

ABRAHAMS, J. P., A. R. LESLIE, R. LUTTER and J. E. WALKER, 1994 Structure at 2.8 Å resolution of F_1-ATPase from bovine heart mitochondria. Nature **370:** 621–628.

ARNHEIM, N., and G. CORTOPASSI, 1992 Deleterious mitochondrial DNA mutations accumulate in aging human tissues. Mutat. Res. **275:** 157–167.

ASCHENBRENNER, M., D. M. MUELLER, R. ZAK and R. J. WIESNER, 1993 Increased expression of F_1-ATP synthase subunits in yeast strains carrying point mutations which destabilize the β subunit. FEBS Lett. **323:** 27–30.

AUSUBEL, F. M., R. BRENT, R. E. KINGSTON, D. D. MOORE, D. D. SEIDMAN *et al.*, 1994 *Current Protocols in Molecular Biology.* Green Publishing Associates/Wiley-Interscience, New York.

BAKHTIARI, N., J. LAI-ZHANG, B. YAO and D. M. MUELLER, 1999 Structure/function of the β-barrel domain of F_1-ATPase in the yeast *Saccharomyces cerevisiae.* J. Biol. Chem. **273:** 16363–16369.

BENEL, L., X. RONOT, J. C. MOUNOLOU, F. GAUDEMER and M. ADOLPHE, 1989 Compared flow cytometric analysis of mitochondria using 10-n-nonyl acridine orange and rhodamine 123. Basic Appl. Histochem. **33:** 71–80.

BODNAR, A. G., M. OUELLETTE, M. FROLKIS, S. E. HOLT, C. P. CHIU *et al.*, 1998 Extension of life-span by introduction of telomerase into normal cells. Science **279:** 349–352.

BOYER, P. D., 1997 The ATP synthase—a splendid molecular machine. Annu. Rev. Biochem. **66:** 717–749.

BUCHET, K., and C. GODINOT, 1998 Functional F_1-ATPase essential in maintaining growth and membrane potential of human mitochondrial DNA-depleted ρ^0 cells. J. Biol. Chem. **273:** 22983–22989.

CHEN, X. J., and G. D. CLARK-WALKER, 1996 The mitochondrial genome integrity gene, *MGI1*, of *Kluyveromyces lactis* encodes the β-subunit of F_1-ATPase. Genetics **144:** 1445–1454.

CONRAD-WEBB, H., and R. A. BUTOW, 1995 A polymerase switch in the synthesis of rRNA in *Saccharomyces cerevisiae.* Mol. Cell. Biol. **15:** 2420–2428.

COSSARIZZA, A., M. BACCARANI-CONTRI, G. KALASHNIKOVA and C. FRANCESCHI, 1993 A new method for the cytofluorimetric analysis of mitochondrial membrane potential using the J-aggregate forming lipophilic cation 5,5′,6,6′-tetrachloro-1,1′,3,3′-tetraethylbenzimidazolcarbocyanine iodide (JC-1). Biochem. Biophys. Res. Commun. **197:** 40–45.

D'MELLO, N. P., and S. M. JAZWINSKI, 1991 Telomere length constancy during aging of *Saccharomyces cerevisiae.* J. Bacteriol. **173:** 6709–6713.

DUPONT, C.-H., J. P. MAZAT and B. GUERIN, 1985 The role of adenine nucleotide translocation in the energization of the inner membrane of mitochondria isolated from ρ^+ and ρ^0 strains of *Saccharomyces cerevisiae.* Biochem. Biophys. Res. Commun. **132:** 1116–1123.

EGILMEZ, N. K., and S. M. JAZWINSKI, 1989 Evidence for the involvement of a cytoplasmic factor in the aging of the yeast *Saccharomyces cerevisae.* J. Bacteriol. **171:** 37–42.

FINCH, C. E., 1990 *Longevity, Senescence, and the Genome.* University of Chicago Press, Chicago.

GANCEDO, C., and R. SERRANO, 1989 Energy-yielding metabolism, pp. 205–259 in *The Yeasts, Metabolism and Physiology of Yeasts,* Vol. 3, Ed. 2, edited by A. H. ROSE and J. S. HARRISON. Academic Press, London.

JAZWINSKI, S. M., 1993 The genetics of aging in the yeast *Saccharomyces cerevisiae.* Genetica **91:** 35–51.

JAZWINSKI, S. M., 1996 Longevity, genes, and aging. Science **273:** 54–59.

JAZWINSKI, S. M., 2001 Modern approaches to the mechanisms of aging: molecular genetics and genomics, pp. 161–193 in *Modern Topics in the Biology of Aging,* edited by V. J. CRISTOFALO and R. ADELMAN. Springer, New York.

KENNEDY, B. K., N. R. AUSTRIACO and L. GUARENTE, 1994 Daughter cells of *Saccharomyces cerevisiae* from old mothers display a reduced life span. J. Cell Biol. **127:** 1985–1993.

KIM, S., B. VILLEPONTEAU and S. M. JAZWINSKI, 1996 Effect of replicative age on transcriptional silencing near telomeres in *Saccharomyces cerevisiae.* Biochem. Biophys. Res. Commun. **219:** 370–376.

Kim, S., A. Benguria, C.-Y. Lai and S. M. Jazwinski, 1999 Modulation of life-span by histone deacetylase genes in *Saccharomyces cerevisiae*. Mol. Biol. Cell **10:** 3125–3136.

Kirchman, P. A., S. Kim, C.-Y. Lai and S. M. Jazwinski, 1999 Interorganelle signaling is a determinant of longevity in *Saccharomyces cerevisiae*. Genetics **152:** 179–190.

Klass, M. R., 1983 A method for the isolation of longevity mutants in the nematode *Caenorhabditis elegans* and initial results. Mech. Ageing Dev. **22:** 279–286.

Kolarov, J., N. Kolarova and N. Nelson, 1990 A third ADP/ATP translocator gene in yeast. J. Biol. Chem. **265:** 12711–12716.

Kováčová, V., J. Irmlerová and L. Kovač, 1968 Oxidative phosphorylation in yeast. IV. Combination of a nuclear mutation affecting oxidative phosphorylation with cytoplasmic mutation to respiratory deficiency. Biochim. Biophys. Acta **162:** 157–163.

Lai-Zhang, J., Y. Xiao and D. M. Mueller, 1999 Epistatic interactions of deletion mutants in the genes encoding the F_1-ATPase in yeast *Saccharomyces cerevisiae*. EMBO J. **18:** 58–64.

Laun, P., A. Pichova, F. Madeo, J. Fuchs, A. Ellinger *et al.*, 2001 Aged mother cells of *Saccharomyces cerevisiae* show markers of oxidative stress and apoptosis. Mol. Microbiol. **39:** 1166–1173.

Liang, Y., and S. H. Ackerman, 1996 Characterization of mutations in the β subunit of the mitochondrial F_1-ATPase that produce defects in enzyme catalysis and assembly. J. Biol. Chem. **271:** 26522–26528.

Lin, Y. J., L. Seroude and S. Benzer, 1998 Extended life-span and stress resistance in the *Drosophila* mutant *methuselah*. Science **282:** 943–946.

Lundblad, V., and J. W. Szostak, 1989 A mutant with a defect in telomere elongation leads to senescence in yeast. Cell **57:** 633–643.

Mortimer, R. K., and J. R. Johnston, 1959 Life span of individual yeast cells. Nature **183:** 1751–1752.

Müller, I., M. Zimmermann, D. Becker and M. Flömer, 1980 Calendar life span versus budding life span of *Saccharomyces cerevisiae*. Mech. Ageing Dev. **12:** 47–52.

Rose, M. R., 1991 *Evolutionary Biology of Aging*. Oxford University Press, New York.

Rose, M. D., P. Novick, J. H. Thomas, D. Botstein and G. R. Fink, 1987 A *Saccharomyces cerevisiae* genomic plasmid bank based on a centromere-containing shuttle vector. Gene **60:** 237–243.

Shen, H., A. Sosa-Peinado and D. M. Mueller, 1996 Intragenic suppressors of P-loop mutations in the β-subunit of the mitochondrial ATPase in the yeast *Saccharomyces cerevisiae*. J. Biol. Chem. **271:** 11844–11851.

Sikorski, R. S., and P. Hieter, 1989 A system of shuttle vectors and yeast host strains designed for efficient manipulation of DNA in *Saccharomyces cerevisiae*. Genetics **122:** 19–27.

Sil, A., and I. Herskowitz, 1996 Identification of asymmetrically localized determinant, Ash1p, required for lineage-specific transcription of the yeast *HO* gene. Cell **84:** 711–722.

Sinclair, D. A., K. Mills and L. Guarente, 1998 Molecular mechanisms of yeast aging. Trends Biochem. Sci. **23:** 131–134.

Smith, J. R., and O. M. Pereira-Smith, 1996 Replicative senescence: implications for in vivo aging and tumor suppression. Science **273:** 63–67.

Strathern, J. N., and I. Herskowitz, 1979 Asymmetry and directionality in production of new cell types during clonal growth: the switching pattern of homothallic yeast. Cell **17:** 371–381.

Wallace, D. C., 1999 Mitochondrial diseases in man and mouse. Science **283:** 1482–1488.

Winston, F., 1994 Mutagenesis of yeast cells, p. 13.3.1 in *Current Protocols in Molecular Biology*, Vol. 2, edited by F. M. Ausubel, R. Brent, R. E. Kingston, D. D. Moore, D. D. Seidman *et al.* Green Publishing Associates/Wiley-Interscience, New York.

Yaffe, M. P., 1999 The machinery of mitochondrial inheritance and behavior. Science **283:** 1493–1497.

Communicating editor: M. Johnston